R. K. Bolingbroke and J. E. King**

A Comparison of Long and Short Fatigue Crack Growth in a High Strength Aluminium Alloy

REFERENCE Bolingbroke, R. K. and King, J. E., **A Comparison of Long and Short Fatigue Crack Growth in a High Strength Aluminium Alloy**, *The Behaviour of Short Fatigue Cracks* (Edited by K. J. Miller and E. R. de los Rios) 1986, Mechanical Engineering Publications, London, pp. 101–114.

ABSTRACT The behaviour of 'microstructurally short' fatigue cracks (20–100 μm in length) in the high strength aluminium alloy, 7010, has been investigated, in an under-aged and an over-aged condition, at the same strength level, to determine the influence of slip and precipitate distribution.

The results of the short crack propagation tests, at 20°C and $R = 0.1$, are compared with conventional (long) fatigue crack propagation and threshold results under the same conditions, and also with long crack tests carried out at constant maximum applied load but increasing mean stress.

In conventional long crack tests, better crack propagation resistance at low ΔK, and a higher threshold, is associated with the under-aged microstructure. The short cracks are found to propagate at significantly higher rates than the long cracks, at $R = 0.1$, below ΔK values of approximately 4 MPa$\sqrt{m}$. At ΔK levels above 7 MPa$\sqrt{m}$, and crack lengths of around 100 μm, the data from the short crack tests merge with the conventional da/dN vs ΔK data measured at $R = 0.1$. The under-aged microstructure again shows somewhat better behaviour in the short crack tests. When the short crack data are compared with high R ratio long crack results, from the constant maximum load tests, the average crack propagation rates are quite similar.

The differences between the long and short crack propagation behaviour at $R = 0.1$ are attributed partly to the absence of roughness-induced closure effects when the cracks are very short, and also to the effects of the high maximum applied stresses, in short crack tests, on the crack-tip plasticity. This argument is also used to explain the degree of correlation shown between short-crack behaviour at $R = 0.1$ and long crack growth rates at $R > 0.8$.

Introduction

There have been a large number of investigations into the fatigue behaviour of precipitation-hardened aluminium alloys. In general the results of these studies are in agreement in two important areas: those of crack initiation and near-threshold crack propagation.

(1) *Crack initiation*. Peak-aged and over-aged alloys show better resistance to crack initiation in slip bands than under-aged alloys **(1)(2)**.

(2) *Near-threshold crack propagation*. By contrast, under-aged microstructures have better long crack propagation resistance at low stress intensities, and also higher threshold values (ΔK_{th}) than over-aged microstructures **(1)–(6)**.

* Department of Metallurgy and Materials Science, University of Nottingham, University Park, Nottingham NG7 2RD, UK.

Both of these effects have been explained in terms of differences in slip distribution caused by the nature of the dislocation/precipitate interactions in under- and over-aged structures. In the under-aged condition, dislocations are assumed to cut precipitates producing local slip band softening. This makes cross-slip unlikely and so leads to the concentration of deformation into a small number of intense slip bands. In over-aged structures the necessity for dislocations to by-pass particles promotes cross-slip and, hence, a more homogeneous strain distribution.

When these effects occur in the surface of a material, leading up to crack initiation in a slip band, peak- and over-aged materials generate a large number of fine slip bands, whereas the intense slip bands formed in under-aged alloys give rise to large slip offsets at the surface, which in turn lead to easy crack initiation.

For the crack propagation behaviour it is suggested that slip occurring in the plastic zone at the crack tip is more reversible in under-aged structures (**1**)(**3**)(**5**) and this leads to slower crack propagation rates. Hornbogen and Zum Gahr (**5**) propose that, for a crack growing along a single slip band at the crack tip, the crack propagation rate should be proportional to the number of dislocations emitted along a slip plane during the loading half of the fatigue cycle which do not return along the same plane during the unloading half. The number of dislocations which contribute to crack advance in each cycle is thus directly related to heterogeneity of the strain, i.e., the ease of cross-slip.

Another factor which is also likely to be important in near-threshold crack propagation, especially where propagation along slip bands in involved, is roughness-induced crack closure (**7**)(**8**). If slip homogeneity affects the fracture profile, then it will affect the closure contribution (K_{cl}) in the measured ΔK_{th} values, so that differences in K_{cl} with ageing treatment may also provide part of the explanation for the higher threshold values in under-aged microstructures.

The behaviour of 'microstructurally short' (**9**) fatigue cracks is sometimes thought to be more closely related to crack initiation and fatigue or endurance limits, than to long crack propagation (**10**). The object of this work, therefore, was to investigate the effect of ageing treatment on short crack behaviour, a particularly interesting area because of the opposite effects of ageing condition on initiation and on long crack propagation resistance. The alloy used for the investigation was a high strength aluminium alloy, 7010, in an under-aged and an over-aged condition with the same yield strength.

Experimental

The material, aluminium alloy 7010, of the composition given in Table 1, was in the form of rolled plate. Fatigue specimens, in the form of square section bars, were cut with their top faces parallel to the surface of the plate, and their lengths aligned with the rolling direction.

The two heat treatments employed involved the following stages: (i) solution

Table 1 Composition (wt%)

Zn	Mg	Cu	Cr	Zr	Si	Fe	Mn	Al
6.2	2.5	1.7	0.05	0.14	0.07	0.11	0.10	balance

treat, 470°C 1 hr, water quench, (ii) pre-age, 90°C, 8 hrs, (iii) age: either 170°C 1 hr (UA), or 170°C 18 hrs (OA). The ageing times were chosen from an ageing curve of yield stress against time at 170°C, to give an under-aged (UA) and an over-aged (OA) condition with the same yield strength.

Long crack propagation tests were performed on single-edge-notch test pieces, 20 mm × 20 mm × 100 mm, containing central notches, 5 mm deep. The da/dN vs ΔK data were determined using a Mayes servo-controlled electro-hydraulic testing machine operating at 50 Hz, in air at 20°C. Specimens were loaded in four point bending and crack length was monitored continuously using a d.c. potential drop technique. Two types of threshold test were performed, conventional tests at a load ratio (R) of 0.1, in which threshold was approached by a load shedding technique, with load reductions of $\simeq 2$ per cent close to threshold, and constant maximum load tests. In this second type of test, ΔK was reduced towards threshold by increasing the minimum load whilst keeping the maximum load constant. The effect of this is to increase the R ratio as ΔK falls. For these tests, the initial loads were chosen such that threshold was reached at R values of about 0.8.

Unnotched bars, in the same orientation as the notched bars, were used for the short crack tests, with dimensions 12.5 mm × 12.5 mm × 70mm. The surface of these specimens were ground and electropolished, after heat treatment, to ensure a smooth, stress-free surface, and then lightly etched in Keller's reagent. The four point bend loading produced a region on the top surface of the specimen, 10 mm × 12.5 mm, which experienced a constant, maximum value of bending moment. The cracks initiated and grew within this region. Tests were run at a frequency of 10 Hz. (The short crack tests were run at a lower frequency than the threshold tests because of the high loads and short replication intervals. Running the threshold tests at 10 Hz would have produced unacceptably long test durations; however, very little effect of frequency between 10 and 50 Hz is anticipated at 20°C.) Crack growth was monitored using a replication technique (**11**), with replicas being taken every 4000 cycles. The maximum surface stress during these tests was 440 MPa (0.9 σ_y), with $R = 0.1$.

Stress intensity values for the short crack tests were calculated using a calibration for semi-elliptical cracks in pure bending (**12**) assuming a ratio of half surface crack length to crack depth of 0.85. This value was determined from measurement of crack shape for a number of cracks present at the end of tests on the smooth specimens. All the cracks measured were found to be of similar shape in both heat-treatment conditions.

Results

Yield strength

The two conditions, UA and OA, were produced with very similar yield strength levels, between 490 and 495 MPa.

Microstructure

The optical micrographs in Fig. 1(a) and (b) illustrate the pancake grain structure common to both ageing conditions. Grain size ranges in the three sections are: L 100 μm–1 mm, LT 60 μm–200 μm, and ST 10 μm–40 μm. The size of the $MgZn_2$ precipitates (η and η') after the two treatments can be seen in Fig. 2, along with occasional $ZrAl_3$ dispersoid particles.

Fatigue crack growth.

Figure 3 shows da/dN vs ΔK for the OA condition at $R = 0.1$. The additional crack depth scale applies to the 'short crack' results from the smooth specimen tests (solid triangles). The long crack data come down to a threshold value of about 2.7 MPa$\sqrt{m}$. The short crack points are for a single, naturally initiated crack. The dip in the crack growth curve for the short crack at $\approx$ 2 MPa$\sqrt{m}$ or $\approx$ 10 μm crack depth, indicated by an arrowed point, is a position at which the crack tip was held up at an obstacle over many cycles, thus giving a growth rate too low to be plotted within the axes of this figure. For crack depths greater than about 100 μm the long and short crack curves merge. Smaller cracks than this grow in an erratic manner, but at average rates above those of the long cracks, and at ΔK values below the long crack threshold at $R = 0.1$.

In Fig. 4 a comparison is made between the OA and the UA conditions. The UA material has the higher long crack threshold of 3.9 MPa$\sqrt{m}$, although growth rates for both conditions are very similar in the Paris regime, above $\Delta K \approx 6$ MPa$\sqrt{m}$. The short crack data for a single crack in the UA material shows the same type of behaviour as the OA, although average growth rates are slightly lower below $\approx$6 MPa$\sqrt{m}$. This is shown more clearly in Fig. 5, where the scatter bands for data from three cracks in OA specimens and two in UA tests are drawn, much of the data overlaps, but the OA material shows consistently higher maximum and average growth rates.

Figure 4 also shows the long crack thresholds from the constant maximum load tests. These thresholds are at R ratios of slightly above 0.8. The high R thresholds are reduced to 1.4 MPa$\sqrt{m}$ for OA and 2 MPa$\sqrt{m}$ for UA material.

Fractography

The fracture surface morphology in the near-threshold regime for long crack tests in the four combinations of ageing treatment and R ratio is shown in Fig. 6. The crack propagation is of a very similar faceted, crystallographic type in each case.

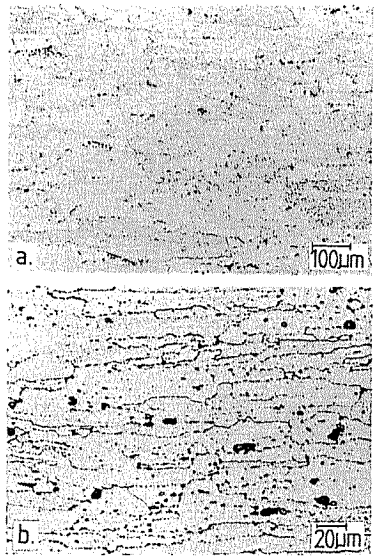

Fig 2 Transmission electron micrographs:
(a) under-aged
(b) over-aged

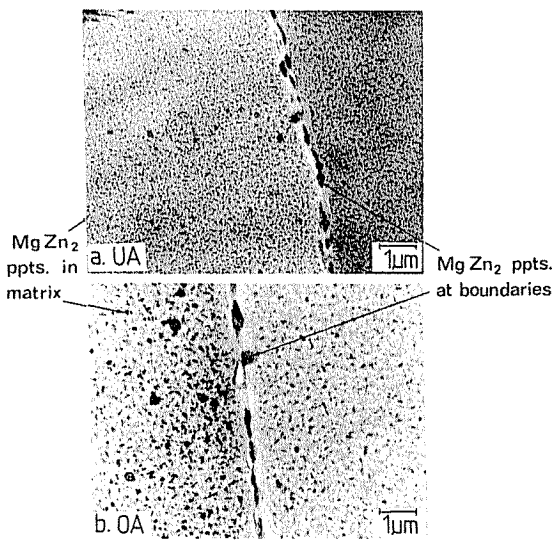

Fig 1 Optical micrographs:
(a) top surface
(b) short-transverse (S-T) section

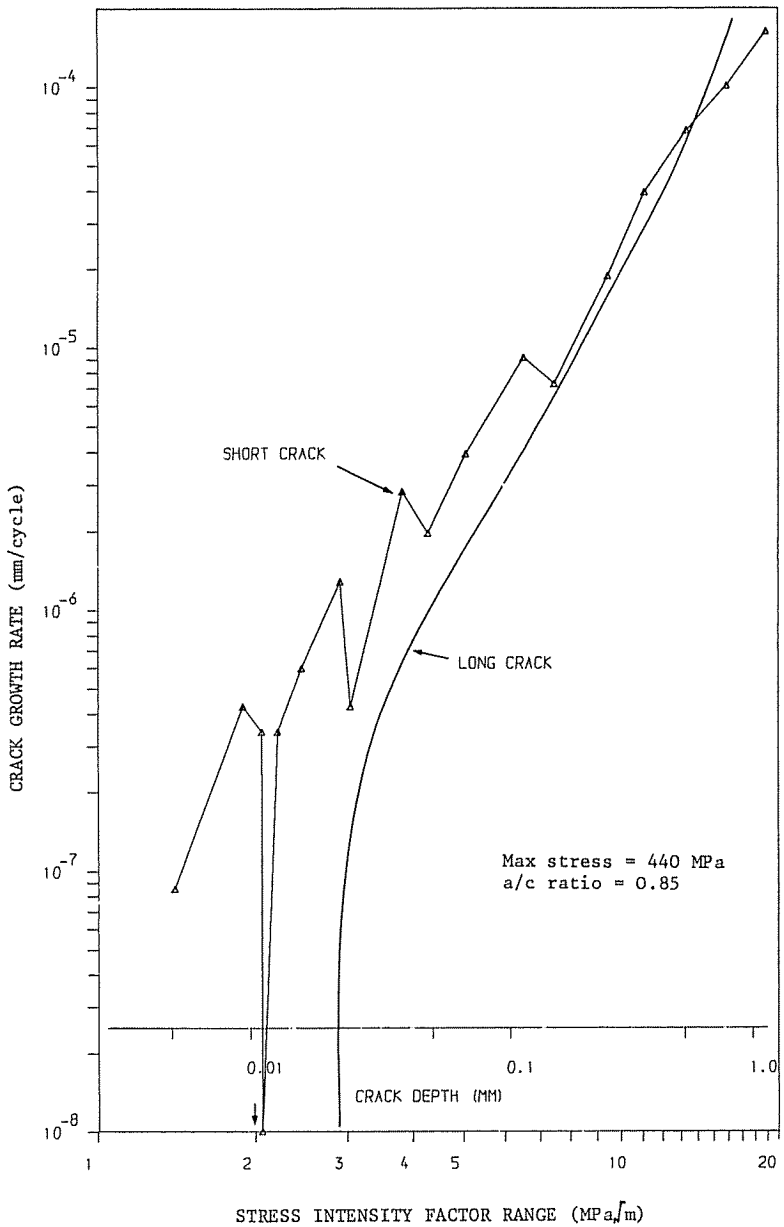

Fig 3 Crack growth rate characteristics. Long and short crack results for over-aged material, air, 20°C, $R = 0.1$

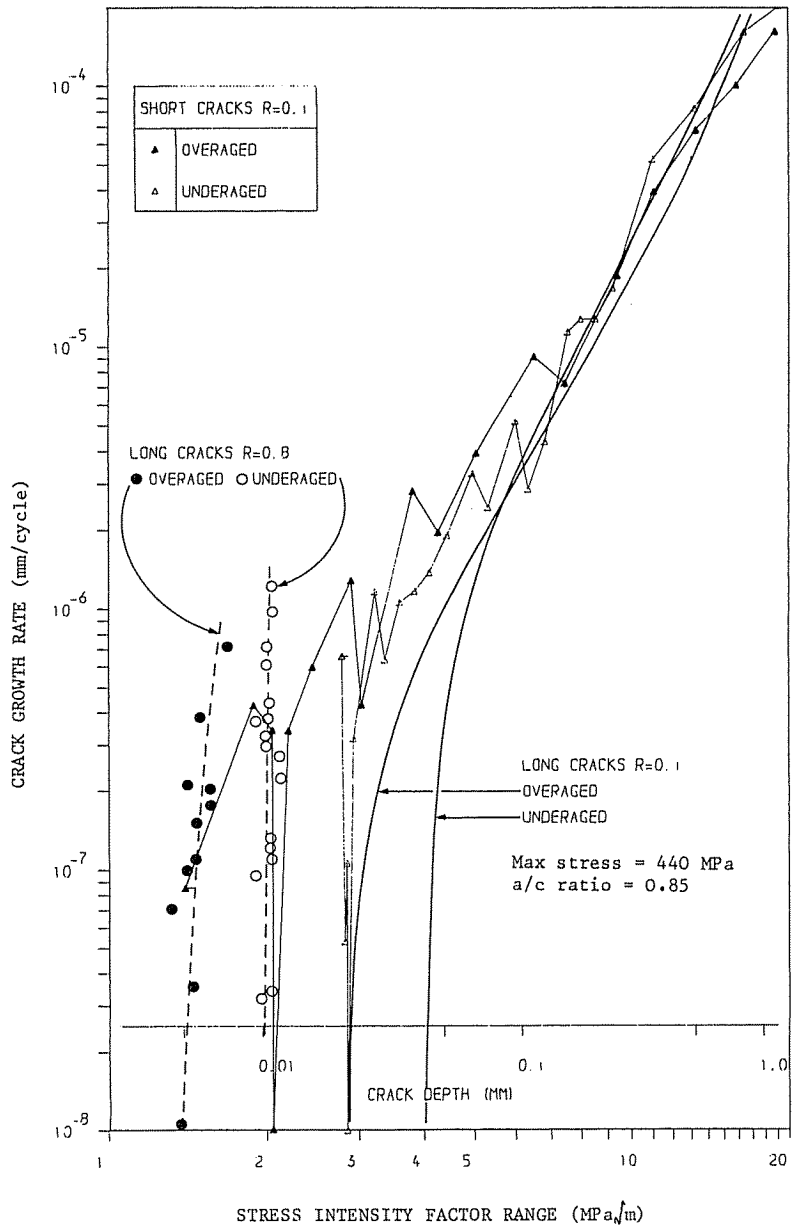

Fig 4 Crack growth rate characteristics in air at 20°C. Long cracks are shown by full lines ($R = 0.1$) and dashed lines ($R = 0.8$). Short cracks are shown by triangular points

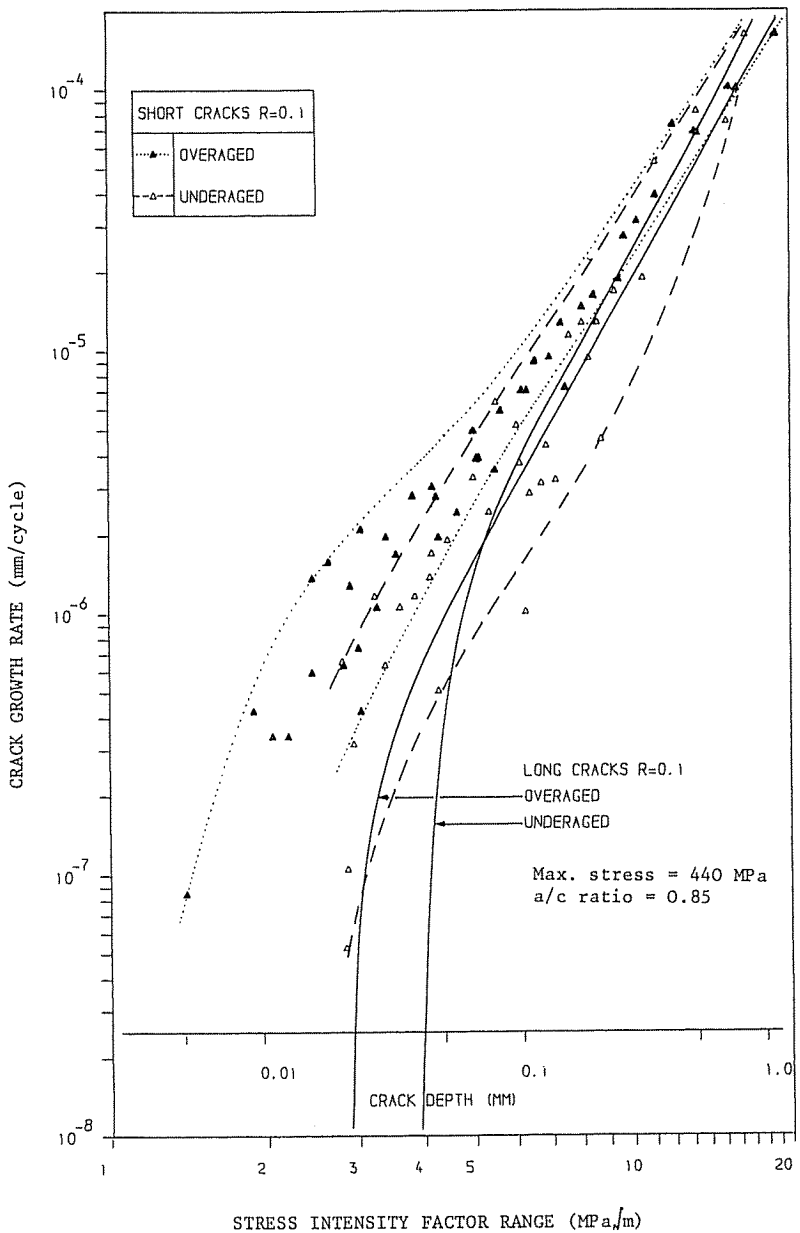

Fig 5 Scatter bands for short crack data representing results from several cracks: $R = 0.1$. Air: 20°C

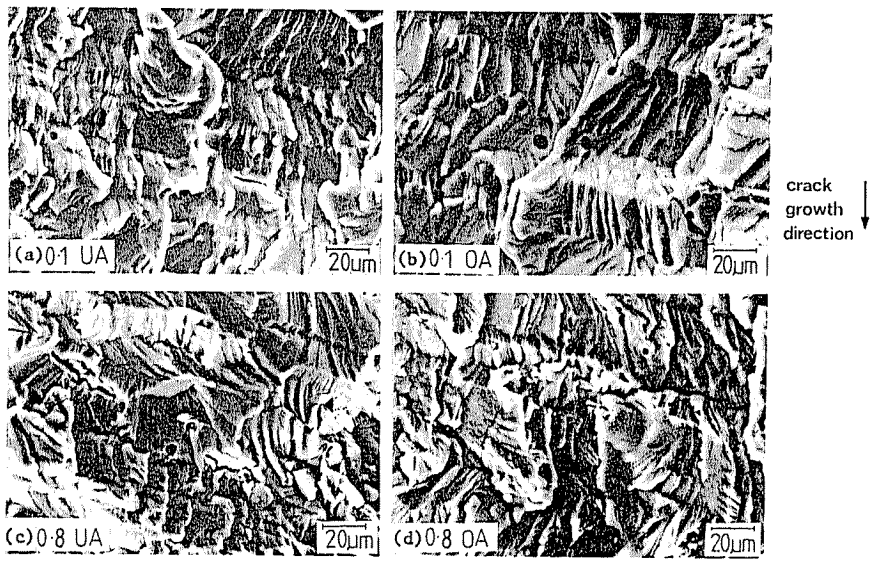

Fig 6 Near-threshold fracture morphology, long cracks: (a) $R = 0.1$ under-aged (b) $R = 0.1$ over-aged (c) $R = 0.8$ under-aged (d) $R = 0.8$ over-aged

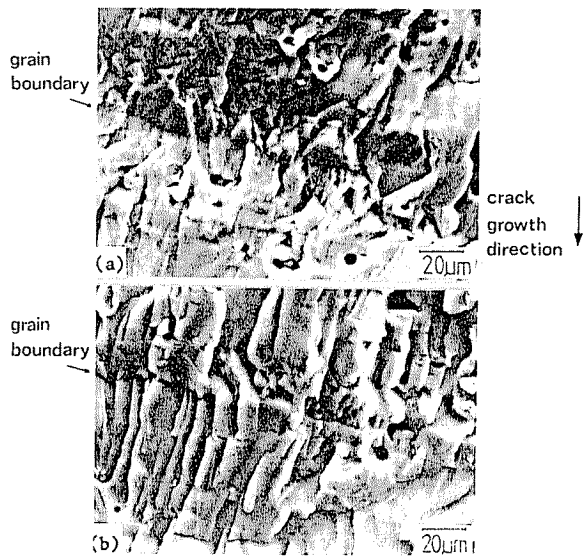

Fig 7 Short crack fracture surfaces (a) $R = 0.1$ under-aged (b) $R = 0.1$ over-aged

Short crack fracture surfaces are illustrated in Fig. 7. Again, the OA and UA fracture paths are very similar, and closely resemble the near-threshold growth in Fig. 6.

Discussion

Behaviour of long, through-thickness cracks

At a load ratio of 0.1 the long crack behaviour shows the normal trend (**1**)–(**6**)(**14**) of higher thresholds and lower near-threshold crack propagation rates in UA material than in OA material.

The threshold values themselves, 3.9 MPa$\sqrt{m}$ (UA) and 2.7 MPa$\sqrt{m}$ (OA), are in good agreement with those from the work of Lankford (**13**) (about 3.8 MPa$\sqrt{m}$) and Suresh *et al.* (**14**) (3.7 MPa$\sqrt{m}$) for under-aged 7075, a similar high strength aluminium alloy, and Suresh *et al.*'s (**14**) value of 2.6 MPa$\sqrt{m}$ for over-aged 7075.

The faceted nature of the near-threshold fracture surfaces in both conditions (Fig. 6) suggests that there will be a significant asymmetrical shear component in crack-tip deformation. This will introduce a degree of mismatch between the two fracture faces and so there will be a roughness-induced closure contribution to the threshold value at $R = 0.1$.

Long crack behaviour at high R will be free of roughness-induced closure effects, because of the larger crack openings involved (**14**)(**15**), so, since the mechanism of crack propagation is the same at $R = 0.1$ and $R = 0.8$ (Fig. 6), the R = 0.8 threshold values can be taken as intrinsic material thresholds. These will be equal to the effective crack tip stress intensity ranges (ΔK_{eff}) at threshold in the $R = 0.1$ tests. The measured values of 2 MPa$\sqrt{m}$ (UA) and 1.4 MPa$\sqrt{m}$ (OA) are again in good agreement with those of Suresh *et al.* (**4**) in 7075, of 1.7 MPa$\sqrt{m}$ (UA) and 1.2 MPa$\sqrt{m}$ (OA).

The superior near-threshold crack propagation resistance of the UA condition observed at $R = 0.1$ persists, in the absence of roughness induced closure, at $R = 0.8$. This suggests that it is due to a difference in the material's inherent resistance to fatigue, perhaps due to increased slip reversibility, rather than a mechanical effect such as a difference in closure behaviour. Suresh *et al.*'s (**14**) proposal that the improved resistance of UA material is due to increased crack deflection does not seem to apply in the present case where the fracture mode in both UA and OA material is very similar, although increased crack deflection might also be a slip reversibility effect.

Comparison of long and short crack behaviour

The propagation rates of short, semi-elliptical cracks in this alloy are greater than those of long, through-thickness cracks at equivalent linear elastic ΔK values and $R = 0.1$, despite a similar fracture mode (Figs 6 and 7). This observation is in agreement with the early work of Pearson (**16**) and more

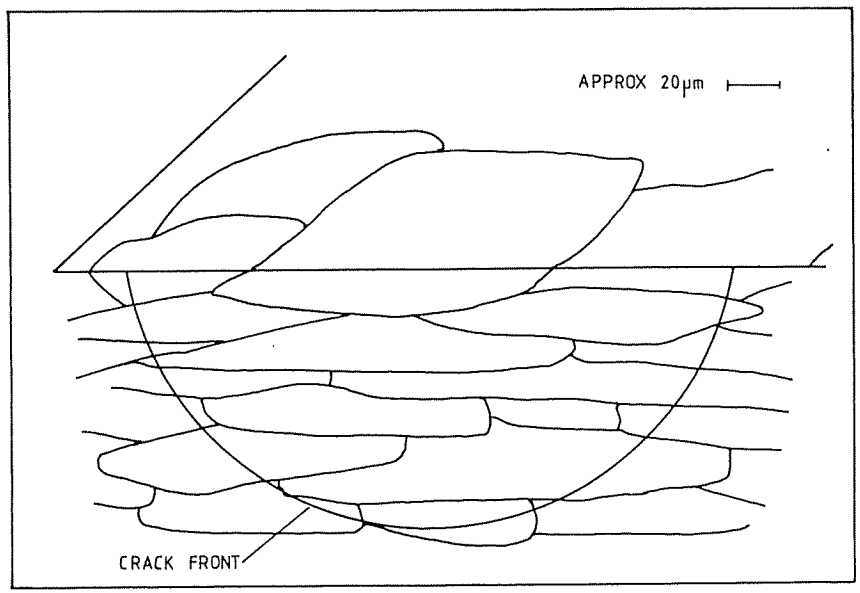

Fig 8 Schematic diagram showing relationship between crack front and grain distribution

recent studies of Morris and co-workers (**17**)(**18**) and of Lankford (**13**), on aluminium alloys.

There has been some discussion about the improper use of linear elastic ΔK to plot short crack data. It is used here, alongside a crack depth scale for the semi-elliptical cracks, for the important reason tht it shows when the cracks in the smooth specimen tests start to behave like long, through-thickness cracks. This occurs for crack depths greater than about 100 μm for both OA and UA conditions. The grain size in the S–T orientation (Fig. 1(b)) is between 10 and 40 μm, so at this stage the crack front will be sampling somewhere between 5 and 20 grains (Fig. 8) and an averaging of crack growth behaviour results.

Once the data from the two types of test have merged (Figs 3 and 4), the agreement between the growth rates form the semi-elliptical cracks and the through-thickness cracks is very good, indicating that, in the range of ΔK involved ($\approx$ 7 to 20 MPa$\sqrt{m}$) there is no crack shape effect on fatigue crack propagation behaviour, if an appropriate K calibration is used. This confirms the work of Pickard, Brown and Hicks (**19**) on crack shape effects in Ni-base and titanium alloys.

It has been suggested that some of the difference between the behaviour of long and short cracks at low ΔK is due to the absence of roughness-induced closure effects when the crack is only of the order of one or two grains in length (**9**)(**20**). It is therefore appropriate to compare short crack data with closure-free long crack results, i.e., ΔK_{eff} values. This comparison can be seen in Fig. 4,

where long crack, high R thresholds are plotted in addition to long and short crack results at $R = 0.1$. Very few of the short crack data appear below the long crack threshold at $R = 0.8$, however, this may simply be due to the difficulty in obtaining short crack results below a ΔK of $\approx$1.5 MPa$\sqrt{m}$ as the inclusions at which the cracks initiated in the present tests were usually several microns in diameter. Further work at lower stress levels and longer test durations is needed to obtain such data. Nevertheless, when compared with closure-free long crack data, very little of the short crack growth seems anomalously fast, suggesting that the absence of roughness induced closure for short cracks does contribute to their high average growth rates.

Another reason for comparing short crack results with high R long crack data is the suggestion, put forward by Brown *et al.* (**20**) that the apparent inability of short cracks to close, even at low R, lies in the extent of crack tip plasticity generated by the high top surface stresses in the short crack test-pieces. They argue that a large maximum plastic zone size is produced, due to the high maximum stress, combined with small reverse plastic zone becaue of the lack of gross yielding on unloading. Thus, it is as if the crack is growing at a high value of R, compared with a simple linear elastic analysis. This should also lead to larger crack openings for short cracks than predicted from linear elastic fracture mechanics, as has been reported by Chan and Lankford (**21**).

The short crack in the smooth bend specimen is growing, effectively, at high R. In the Paris regime long crack data are relatively insensitive to R ratio, because of the declining importance of closure effects as symmetrical, continuum deformation takes over at the crack tip and the fracture surfaces become flatter. Thus the short crack data would be expected to merge with the $R = 0.1$ long crack data in the Paris regime, as the experimental results show. There may also be an additional effect in the smooth bend specimen. As the crack lengthens the effective value of R, at the deepest point of the crack, may decrease as the fibre stress in the specimen falls on moving away from the top surface. This would also cause the short crack data to move from the $R = 0.8$ long crack curve towards the $R = 0.1$ long crack results as crack depth increases. This might produce a slight difference in the crack lengths at which long and short crack data merge, depending on whether the short crack tests are carried out in bend or in tension.

Aspects of short crack growth

The irregular nature of the short crack growth appears to be closely associated with the grain size and, therefore, interactions between the crack tip and grain boundaries. This is seen clearly in Fig. 3 for the OA material, where dips in growth rate occur for the short crack at depths of $\approx$10, 30, and 50 μm, corresponding to the grain size of between 10 and 40 μm in the S–T orientation (Fig. 1(b)). The resulting changes in orientation of the fracture path at each grain boundary can be seen on the fracture surface in Fig. 7(b). This is in

agreement with many previous observations (**9**)(**13**)(**17**)(**18**) and has been interpreted as being due to the difficulty of reinitiating slip in a new orientation in the next grain.

Such observations might lead one to expect that the crack shape for the short cracks would be related to the grain shape, such that cracks growing through long, thin pancake grains would be shallow cracks with large surface length to depth ratios. However, the cracks observed here were almost semicircular, over a wide range of crack lengths, as were those observed by Lankford in 7075 (**13**) at crack depths as small as 10 μm. The consistent crack shape, maintained from within the first grain through to the long crack regime where the crack front spans numerous grains, suggests that it is appropriate to use a single controlling parameter to describe crack propagation over the whole range of crack length.

The UA condition shows better short crack propagation resistance than the OA condition, in common with the long crack results and in contrast to reports of crack initiation resistance (**1**)(**2**). This reinforces the view that it is an inherent microstructural property, such as slip reversibility in the plastic zone, that causes the effect.

Conclusions

(1) Short fatigue cracks (depths $<$100 μm) in under- and over-aged 7010 propagate faster than long through-thickness cracks at the same apparent applied ΔK, and $R = 0.1$.

(2) Short crack growth rates at $R = 0.1$ are bounded by the long crack data measured at high R, over the range of crack length and ΔK it has been possible to obtain in these tests, but lie above the long crack growth rates at $R = 0.1$.

(3) Long and short fatigue cracks at low ΔK produce similar, faceted fracture surfaces, indicating that the same crack propagation mechanism is operative, despite differences in propagation rate.

(4) Under-aged 7010 shows significantly better crack propagation resistance than over-aged 7010 in the near threshold regime for long cracks. Higher threshold values are obtained in under-aged 7010, even when roughness-induced closure effects are eliminated. Short crack propagation resistance also appears to be slightly better in the under-aged condition, with consistently higher average and maximum growth rates in over-aged material in the short crack regime.

(5) The discontinuous nature of short crack growth is associated with the grain size of the material.

(6) There is no crack shape effect on fatigue crack propagation in under- and over-aged 7010 between ΔK values of 7 and 20 MPa$\sqrt{m}$. Semi-elliptical and through-thickness cracks propagate at the same rates in this range, with the same fracture mode.

Acknowledgements

The authors wish to thank Professor J. S. L. Leach for provision of laboratory facilities, Dr R. N. Wilson and Dr C. W. Brown for helpful discussions, and Mr K. Dinsdale and Mr F. Garlick for assistance with electron microscopy and mechanical testing. This work has been carried out with the support of the procurement Executive, Ministry of Defence.

References

(1) GYSLER, A., LINDIGKEIT, J., and LUTJERING, G. (1979) Correlation between microstructure and fatigue fracture, *Proceedings of ICSMA5*, Aachen, p. 1113.
(2) MUGHRABI, H. (1983) Deformation of multi-phase and particle-containing materials, *Proceedings of 4th Riso Int. Symp. on Met. and Mat. Sci.* Denmark, p. 65.
(3) LINDIGKEIT, J., GYSLER, A. and LUTJERING, G. (1981) The effect of microstructure on the fatigue crack propagation behaviour of an Al–Zn–Mg–Cu alloy, *Metal. Trans*, **12A**, 1613–1619.
(4) GARRETT, G. G. and KNOTT, J. F. (1975) Crystallographic fatigue crack growth in Al alloys, *Acta Met.*, **23**, 841–848.
(5) HORNBOGEN, E. and ZUM GAHR, K. H. (1976) Microstructure and fatigue crack growth in a γ-Fe–Ni aluminium alloy, *Acta Met.*, **24**, 581–592.
(6) ANTOLOVICH, S. D. and JAYARAMAN, N. (1980) Fatigue: environment and temperature effects, *Proceedings of 27th Sagamore Army Materials Research Conf.*, p. 119.
(7) WALKER, N. and BEEVERS, C. J. (1979) A fatigue crack closure mechanism in titanium, *Fatigue Engng Mater. Structures*, **1**, 135–148.
(8) RITCHIE, R. O. and SURESH, S. (1982) Some considerations on fatigue crack closure at threshold stress intensity due to fracture surface morphology, *Met. Trans*, **13A**, 937–940.
(9) RITCHIE, R. O. and SURESH, S. (1982) Behaviour of short cracks in airframe components, *Proceedings of 55th AGARD Struct. and Mats. Panel meeting*, Canada.
(10) MILLER, K. J. (1982) The short crack problem, *Fatigue Engng Mater. Structures*, **5**, 223–232.
(11) BROWN, C. W. and SMITH, G. C. (1982) A two stage plastic replication technique for monitoring fatigue crack initiation and early fatigue crack growth, *Advances in crack length measurement* (EMAS), p. 41.
(12) ROOKE, D. P. and CARTWRIGHT, D. J. (1976) *Compendium of stress intensity factors* (HMSO, London).
(13) LANKFORD, J. (1982) The growth of small fatigue cracks in 7075-T6 aluminium, *Fatigue Engng Mater. Structures*, **5**, 233–248.
(14) SURESH, S., VASUDEVAN, A. K., and BRETZ, P. E. (1984) Mechanisms of slow fatigue crack growth in aluminium alloys: The role of microstructure and environment, *Met. Trans.*, **15A**, 369–379.
(15) VENABLES, R. A., HICKS, M. A., and KING, J. E. (1984) Influence of stress ratio on fatigue threshold and structure sensitive crack growth in Ni base superalloys, *Fatigue crack growth threshold concepts* (ASM), p. 341.
(16) PEARSON, S. (1975) Initiation of fatigue cracks in commercial aluminium alloys and the subsequent propagation of very short cracks, *Engng Fracture Mech*, **7**, 235–247.
(17) MORRIS, W. L., JAMES, M. R., and BUCK, O. (1981) Growth rate models for short surface cracks in Al 2219–T851, *Met. Trans*, **12A**, 57–64.
(18) ZUREK, A. K., JAMES, M. R., and MORRIS, W. L. (1983) The effect of grain size on fatigue growth of short cracks, *Met. Trans*, **14A**, 1697–1705.
(19) PICKARD, A. C., BROWN, C. W., and HICKS, M. A. (1983) The development of advanced specimen testing and analysis techniques applied to fracture mechanics lifting of gas turbine components, *Advances in life prediction methods* (ASME), p. 173.
(20) BROWN, C. W., KING, J. E., and HICKS, M. A. (1984) The effects of microstructure on long and short fatigue crack growth in Ni-base superalloys, *Met. Sci.*, **18**, 374–380.
(21) CHAN, K. S. and LANKFORD, J. (1983) A crack tip strain model for the growth of small fatigue cracks, *Scripta Met.*, **17**, 529–532.